

Homa Ashrafpour, Ning Huang, Peter C. Neligan, Christopher R. Forrest, Patrick D. Addison, Michael A. Moses, Ronald H. Levine and Cho Y. Pang
Am J Physiol Heart Circ Physiol 286:946-954, 2004. First published Nov 26, 2003;
doi:10.1152/ajpheart.00901.2003

You might find this additional information useful...

This article cites 44 articles, 21 of which you can access free at:

<http://ajpheart.physiology.org/cgi/content/full/286/3/H946#BIBL>

This article has been cited by 6 other HighWire hosted articles, the first 5 are:

Peptide Hormone Regulation of Angiogenesis

C. Clapp, S. Thebault, M. C. Jeziorski and G. Martinez De La Escalera
Physiol Rev, October 1, 2009; 89 (4): 1177-1215.

[\[Abstract\]](#) [\[Full Text\]](#) [\[PDF\]](#)

Design of Clinical Trials of Radiation Combined with Antiangiogenic Therapy

S. Senan and E. F. Smit
Oncologist, April 1, 2007; 12 (4): 465-477.

[\[Abstract\]](#) [\[Full Text\]](#) [\[PDF\]](#)

Efficacy and mechanism of adenovirus-mediated VEGF-165 gene therapy for augmentation of skin flap viability

N. Huang, A. Khan, H. Ashrafpour, P. C. Neligan, C. R. Forrest, C. D. Kontos and C. Y. Pang
Am J Physiol Heart Circ Physiol, July 1, 2006; 291 (1): H127-H137.

[\[Abstract\]](#) [\[Full Text\]](#) [\[PDF\]](#)

Prolactins Are Natural Inhibitors of Angiogenesis in the Retina

J. Aranda, J. C. Rivera, M. C. Jeziorski, J. Riesgo-Escovar, G. Nava, F. Lopez-Barrera, H. Quiroz-Mercado, P. Berger, G. Martinez de la Escalera and C. Clapp
Invest. Ophthalmol. Vis. Sci., August 1, 2005; 46 (8): 2947-2953.

[\[Abstract\]](#) [\[Full Text\]](#) [\[PDF\]](#)

Evolution of a "falx lunatica" in demarcation of critically ischemic myocutaneous tissue

Y. Harder, M. Amon, M. Georgi, A. Banic, D. Erni and M. D. Menger
Am J Physiol Heart Circ Physiol, March 1, 2005; 288 (3): H1224-H1232.

[\[Abstract\]](#) [\[Full Text\]](#) [\[PDF\]](#)

Updated information and services including high-resolution figures, can be found at:

<http://ajpheart.physiology.org/cgi/content/full/286/3/H946>

Additional material and information about *AJP - Heart and Circulatory Physiology* can be found at:

<http://www.the-aps.org/publications/ajpheart>

This information is current as of November 25, 2009 .

Vasodilator effect and mechanism of action of vascular endothelial growth factor in skin vasculature

Homa Ashrafpour,¹ Ning Huang,¹ Peter C. Neligan,^{1,2} Christopher R. Forrest,^{1,2} Patrick D. Addison,^{1,2} Michael A. Moses,^{1,2} Ronald H. Levine,² and Cho Y. Pang^{1–3}

¹Research Institute, The Hospital for Sick Children, and Departments of ²Surgery and ³Physiology, University of Toronto, Toronto, Ontario, Canada M5G 1X8

Submitted 18 September 2003; accepted in final form 20 November 2003

Ashrafpour, Homa, Ning Huang, Peter C. Neligan, Christopher R. Forrest, Patrick D. Addison, Michael A. Moses, Ronald H. Levine, and Cho Y. Pang. Vasodilator effect and mechanism of action of vascular endothelial growth factor in skin vasculature. *Am J Physiol Heart Circ Physiol* 286: H946–H954, 2004. First published November 26, 2003; 10.1152/ajpheart.00901.2003.—Various laboratories have reported that local subcutaneous or subdermal injection of VEGF₁₆₅ at the time of surgery effectively attenuated ischemic necrosis in rat skin flaps, but the mechanism was not studied and enhanced angiogenesis was implicated. In the present study, we used the clinically relevant isolated perfused 6 × 16-cm pig buttock skin flap model to 1) test our hypothesis that VEGF₁₆₅ is a potent vasodilator and acute VEGF₁₆₅ treatment increases skin perfusion; and 2) investigate the mechanism of VEGF₁₆₅-induced skin vasorelaxation. We observed that VEGF₁₆₅ (5 × 10⁻¹⁶–5 × 10⁻¹¹ M) elicited a concentration-dependent decrease in perfusion pressure (i.e., vasorelaxation) in skin flaps precontracted with a submaximal concentration of norepinephrine (NE), endothelin-1, or U-66619. The VEGF₁₆₅-induced skin vasorelaxation was confirmed using a dermo-fluorometry technique for assessment of skin perfusion. The vasorelaxation potency of VEGF₁₆₅ in NE-precontracted skin flaps (pD₂ = 13.57 ± 0.31) was higher (P < 0.05) than that of acetylcholine (pD₂ = 7.08 ± 0.24). Human placental factor, a specific VEGF receptor-1 agonist, did not elicit any vasorelaxation effect. However, a specific antibody to VEGF receptor-2 (1 μg/ml) or a specific VEGF receptor-2 inhibitor (5 × 10⁻⁶ M SU-1498) blocked the vasorelaxation effect of VEGF₁₆₅ in NE-precontracted skin flaps. These observations indicate that the potent vasorelaxation effect of VEGF₁₆₅ in the skin vasculature is initiated by the activation of VEGF receptor-2. Furthermore, using pharmacological probes, we observed that the postreceptor signaling pathways of VEGF₁₆₅-induced skin vasorelaxation involved activation of phospholipase C and protein kinase C, an increase in inositol 1,4,5-trisphosphate activity, release of the intracellular Ca²⁺ store, and synthesis/release of endothelial nitric oxide, which predominantly triggered the effector mechanism of VEGF₁₆₅-induced vasorelaxation. This information provides, for the first time, an important insight into the mechanism of VEGF₁₆₅ protein or gene therapy in the prevention/treatment of ischemia in skin flap surgery and skin ischemic diseases.

VEGF₁₆₅ receptors; signaling pathways; nitric oxide; prostacyclin; skin flap

SKIN FLAPS ARE ROUTINELY USED for coverage of large deep wounds or tissue defects resulting from injury, excision of tumors, ulceration, or congenital malformation. In skin flap surgery, a large piece of skin with subcutaneous tissue is undermined and elevated from a donor site. The skin flap is

immediately transferred and sutured to the nearby wound (i.e., pedicled skin flap surgery) or detached and transferred to a distant site for wound coverage where the artery and vein of the skin flap vascular pedicle are anastomosed to vessels in the recipient site for blood supply (i.e., autogenous skin transplantation or free flap surgery) (5, 11).

Distal ischemic necrosis is the most common clinical complication in pedicled skin flap surgery, but the pathogenic mechanism is unclear. The general consensus is that unpredictable vasospasm, thrombosis, and insufficient vascularity are the main factors in the pathogenesis of distal skin ischemic necrosis in pedicled skin flaps (5). Numerous systemic vasodilator drugs and several antithrombotic drugs and topical vasodilator drugs have been investigated in laboratory animals for augmentation of skin blood flow and viability in pedicled skin flaps by many investigators, but the results thus far are either disappointing, controversial, or very modest at best, and none has reached the clinical trial stage (5, 7, 32). Most if not all systemic vasodilators are not effective in augmentation of skin flap viability probably because they cause systemic hypotension, which is known to be detrimental to skin flap blood flow and viability. Of particular interest are recent publications that reported that acute local VEGF₁₆₅ protein or gene therapy was effective in mitigation of skin flap ischemic necrosis. Specifically, it was reported that local subcutaneous or subdermal injection of VEGF₁₆₅ at the time of flap surgery attenuated skin ischemic necrosis in skin and musculocutaneous flaps in the rat (19, 31, 37). It was also reported that local subcutaneous injection of naked plasmid DNA encoding VEGF₁₆₅ given at the time of surgery or adenovirus encoding the VEGF₁₆₅ gene given at 12 h before skin flap surgery attenuated ischemic necrosis in rat skin flaps (12, 30). The mechanism of acute local VEGF₁₆₅ protein or gene therapy in attenuation of skin ischemic necrosis in flap surgery in these studies was not investigated, but enhanced angiogenesis and/or neovascularization were implicated by these investigators. In our opinion, angiogenesis and neovascularization may not explain the action of acute VEGF₁₆₅ protein or gene therapy in the mitigation of skin flap ischemic necrosis. Specifically, the maximum time for ischemic tolerance in skin flaps is 8–13 h (17), but it may take at least 2 to 3 days for VEGF₁₆₅ to establish angiogenesis or neovascularization (18). Therefore, the critical ischemic time of skin flaps would be surpassed before any benefits can be gained from angiogenesis or neovascularization induced by VEGF₁₆₅ protein or gene therapy started 12 h before or at the

Address for reprint requests and other correspondence: C. Y. Pang, The Hospital for Sick Children, 555 University Ave., Toronto, Ontario, Canada M5G 1X8 (E-mail: pang@sickkids.ca).

The costs of publication of this article were defrayed in part by the payment of page charges. The article must therefore be hereby marked “advertisement” in accordance with 18 U.S.C. Section 1734 solely to indicate this fact.

time of skin flap surgery (12, 19, 30, 31, 37). We hypothesize that not only is VEGF₁₆₅ important in the initiation and progression of angiogenesis and neovascularization but that it also possesses a potent vasodilator effect principally by stimulating synthesis and release of endothelium-derived relaxing factors, which increase blood flow to the hypoperfused skin in the distal portion of the skin flap. This vasodilator effect of VEGF₁₆₅ explains the efficacy of acute VEGF₁₆₅ protein or gene therapy in the augmentation of pedicled skin flap viability. Our hypothesis on the vasodilator effect of VEGF₁₆₅ is supported by other observations showing that acute coronary artery infusion of VEGF₁₆₅ increased coronary blood flow in the pig (23), and VEGF₁₆₅ elicited vasorelaxation in animal and human vascular rings in organ chambers (20–24, 41, 44). At the present time, little is known about the vasodilator effect and mechanism of action of VEGF₁₆₅ in the skin vasculature. Therefore, we planned to test our hypothesis by investigating 1) the vasorelaxation effect of acute VEGF₁₆₅ treatment in the skin vasculature; 2) the receptor and postreceptor signal transduction pathways mediating VEGF₁₆₅-induced vasorelaxation in the skin vasculature; and 3) the effector mechanism associated with VEGF₁₆₅-induced vasorelaxation in the skin vasculature. The isolated perfused pig buttock skin flap model was used in the present study because the vasculature in this skin flap model resembles very closely to that of the human arterial skin flap routinely used in reconstructive surgery (4). The techniques for surgical construction and perfusion of pig arterial island buttock skin flaps have been previously described by us (33–35) and other investigators (27, 39, 40).

MATERIALS AND METHODS

Surgical Procedures

Yorkshire pigs (19.5 ± 1.8 kg, mean ± SD) were used. Skin flaps were harvested under general anesthesia induced by intramuscular ketamine (25 mg/kg) and intravenous pentobarbitone sodium (20–25 mg/kg). General anesthesia was maintained by an intravenous infusion of isotonic saline (2 ml/min) containing pentobarbitone sodium (0.5 mg·kg⁻¹·min⁻¹). A 6 × 16-cm skin flap based on the deep circumflex iliac neurovascular bundle was outlined on both sides of the buttock. These marked skin flaps were incised and completely undermined with all musculocutaneous blood vessels (perforators) tied and/or cauterized carefully. The circumflex iliac neurovascular bundle was dissected and formed the vascular pedicle (~4 cm) of the island buttock skin flap. All side branches of blood vessels of the pedicle were ligated with 4-0 silk sutures and cauterized. Finally, the proximal end of the neurovascular pedicle of the flap was tied with a 2-0 silk suture and then transected. The arterialized island buttock skin flap was freed and used for *in vitro* perfusion as described previously (33–35). The pig was killed with an overdose of intravenous pentobarbitone sodium (100 mg/kg). This animal protocol was approved by The Hospital for Sick Children Animal Care Committee.

Skin Flap Preparation for In Vitro Perfusion

The skin flap was wrapped around a plastic tube (22 cm in length and 1.2 cm in diameter), and the longitudinal edges of the flap were sewn together with 3-0 silk sutures to form a tubed flap. From our previous experience, inclusion of this tube in the tubed skin flap significantly reduced edema formation during 4 to 5 h of *in vitro* perfusion, and water retention was reduced to <10% (33–35). The circumflex iliac artery and one of its veins were cannulated with a 20- and 18-gauge angiocatheter, respectively, for skin flap perfusion. The warm ischemic time required for construction of a tubed skin flap and

cannulation was 20–30 min. We previously demonstrated *in vivo* that this pig skin flap model could tolerate 2 h of primary and 10 h of secondary ischemia without skin ischemic necrosis (14). Therefore, it is unlikely that skin ischemia-reperfusion injury could have taken place in our isolated perfused skin flap model.

Skin Flap Perfusion Technique

Modified Krebs-Henseleit buffer of the following composition (in mM) was used for the perfusate: 100 NaCl, 4.60 KCl, 1.10 NaH₂PO₄, 1.20 MgSO₄, 2.25 CaCl₂, 30 NaHCO₃, 11 glucose, and 2 D-mannitol. Bovine serum albumin (Cohn fraction V) was added to the buffer (65 g/l), which was stirred and filtered (Whatman no. 44) before use. A similar perfusate was used by other investigators in the isolated perfused pig skin flap model (27, 39, 40). Krebs buffer instead of whole blood was chosen as the perfusate to avoid confounding effects of vasoactive substances released by traumatized blood cells.

The commercially available Two-Ten Perfuser (MX International; Aurora, CO) equipped with two reservoirs and a pump with adjustable rates (model 7014, Cole Palmer Instruments; Vernon Hills, IL) was used as a perfusion apparatus. The perfusate was equilibrated in the reservoirs with 95% O₂-5% CO₂ at 38°C and pH 7.35–7.40. The perfusate was kept at 37°C. A three-way connector that linked the tubing from the peristaltic pump to the arterial angiocatheter of the flap permitted a parallel tubing to be connected to a pressure transducer (AB High Performance Pressure Transducer, Data Instruments; Lexington, KY). The transducer output was displayed continuously on a digital monitor (Trendicator II 621A, Doric Scientific; San Diego, CA) and a chart recorder (Lineacorder WR3101, Graphtec). The pump was adjusted to produce a basal perfusion pressure of 35–40 mmHg. Drugs to be studied were infused into the perfusate through a side arm shortly before the perfusate entered the arterial angiocatheter of the skin flap. A thermister probe (YSI Series 400, Yellow Springs Instruments; Yellow Springs, OH) connected to a microcomputer thermometer (Series 084 202, Cole Palmer Instruments) was positioned on the surface of the longitudinal midpoint of the skin flap for continuous monitoring of surface skin temperature, which was kept at ~34°C.

A baseline perfusion pressure of 35–40 mmHg was selected because our past experiments revealed that the pig skin flap was well perfused and oxygenated (33–35). The basal perfusion pressure used by other investigators for perfusion of rabbit ears was 35.8 ± 3.5 mmHg (38). From our past experience, we also noticed that the weights of the 6 × 16-cm buttock skin flaps in pigs weighing 17–22 kg were quite uniform (51 ± 3 g). A pump rate of 1.5–2.0 ml/min would produce a baseline perfusion pressure of 35–40 mmHg. At the beginning of each experiment, a 45-min stabilization period was allowed to establish a steady baseline perfusion pressure at a constant flow rate.

Construction of Concentration-Dependent Vasorelaxation Curves

In all experiments, skin flaps were perfused with Krebs-Henseleit buffer at a constant flow rate throughout each experiment. Norepinephrine (NE), endothelin-1 (ET-1), or the thromboxane A₂ mimetic U-46619 was infused into the perfusate continuously through the side arm to cause a sustained increase in perfusion pressure (i.e., vascular contraction). After the increase in perfusion pressure was stabilized, a cumulative concentration-dependent vasorelaxation curve was constructed by stepwise infusion of a vasodilator drug to the perfusate through the side arm. Each increment (0.5 log) of vasodilator drug was made only after the response to the preceding concentration of drug had stabilized. Vasodilator drugs caused a concentration-dependent decrease in perfusion pressure (i.e., vasorelaxation), and vasorelaxation was expressed as a percentage of the perfusion pressure (contraction) induced by a submaximal dose of NE, ET-1, or U-46619 as described previously (2). When an inhibitor/antagonist was used to block the action of the vasorelaxation drug, it was infused continu-

ously into the perfusate starting 30 min before the beginning of the concentration-dependent relaxation-response experiment.

A least-square best-fit computer program (Prism, GraphPad; San Diego, CA) was used for plotting line graphs for concentration-dependent response curves and for calculation of the concentration of a drug that elicited 50% (EC₅₀) and 100% (EC₁₀₀) of the maximum vasorelaxation. Apparent affinity (pD₂) was calculated as the negative log molar concentration of EC₅₀ (35).

Surface Dermofluorometry Technique for Assessment of Skin Perfusion

The dermofluorometry technique for assessment of in vivo dermal perfusion was validated against the radioactive microsphere technique in the pig skin (43). We adopted this dermofluorometry technique for the assessment of dermal perfusion in isolated perfused pig skin flaps (33). Specifically, confluent circles of 1 cm diameter were marked along the longitudinal midline of the skin flap surface. After the 45-min stabilization period, the background fluorescence in each circular skin area was measured (fluorescence units) using a dermofluorometer (Fluorescan unit, Santa Barbara Technology; Santa Barbara, CA). Fluorescence dye (Diofluor, fluorescein sodium, 100 mg/ml, Dioptic Laboratories; Markham, Ontario, Canada) with a final concentration of 3×10^{-5} M was then infused into the skin flap for 5 min, and fluorescence in each circle was measured again. A washout period of 15 min was allowed, and the background fluorescence was taken again. The drug to be tested was infused into the skin flap. After the perfusion pressure had stabilized subsequent to drug infusion for the study of skin vascular reactivity, fluorescence dye infusion was repeated, and skin fluorescence was measured again. The difference in fluorescence units for each circular skin area between the background and postfluorescence dye infusion was defined as the net fluorescence unit for that area. The total dye fluorescence is the sum of all net fluorescence units measured from all circular skin areas along the midline of the skin flap (43).

Assessment of Stable End Products of Nitric Oxide and PGI₂ in Pig Skin Arteries

The end products of nitric oxide (NO) are nitrite/nitrate (NO₂⁻/NO₃⁻; NO_x). The end product of PGI₂ is 6-keto-PGF_{1α}. The methods for analysis of tissue contents of NO_x and 6-keto-PGF_{1α} were similar to those reported previously (15, 47). Briefly, arteries and veins (~100 mg) dissected from pig skin flaps were homogenized at 4°C in a buffer containing 25 mmol/l Tris·HCl (pH 7.5), 0.5 mmol/l EDTA, and 0.5 mmol/l EGTA and centrifuged at 14,000 g for 15 min. The resulting supernatants were collected as cytosolic fractions for assay of protein content determined by the Bradford method (Bio-Rad), 6-keto-PGF_{1α} using a commercial radioimmunoassay (RIA) kit, and assay of NO_x using the following techniques. The supernatants were loaded to a Centricon YM-30 filter and centrifuged at 4°C to remove substances larger than 30 kDa. NO₂⁻ content was assayed using the Griess reaction. NO₃⁻ content was determined after the conversion of NO₃⁻ to NO₂⁻ with *Aspergillus* nitrate reductase. Tissue NO_x contents are expressed as nanomoles per milligram of protein.

Biochemicals

All chemicals and the antibody to VEGF receptor-2 were purchased from Sigma Chemical (Oakville, Ontario, Canada) except the following: ET-1 was from Peptide International (Louisville, KY), fluorescein dye (100 mg/ml Diofluor) was from Dioptic Laboratory (Markham, Ontario, Canada), injectable NE was from Sabex (Boucherville, Quebec, Canada), *N*-[3-(aminomethyl)-benzyl]-acetamine (1400W) and *N*^ω-propyl-L-arginine (L-NPA) were from Tocris (Ellisville, MO), human placental growth factor (PIGF) and recombinant human VEGF₁₆₅ were from R&D Systems (Minneapolis, MN), SU-1498 was from Calbiochem (San Diego, CA), U-46619 was from

Cayman (Ann Arbor, MI), and RIA kits for 6-keto-PGF_{1α} were from Amersham (Baie d'urfé, Quebec, Canada). Perfusion buffer was made on the day of each experiment using distilled Milli Q water. The freshly made buffer was used to make drug stock solutions, which were stored at 4°C before use. *N*^ω-nitro-L-arginine (L-NNA) was dissolved in 0.5 ml of 0.1 N HCl. The following drugs were dissolved in 0.5 ml of DMSO before being added to the buffer to make stock solutions: 2-aminoethoxydiphenylborate (2-APB), 1,2-bis-(2-amino-phenoxy)ethane-*N,N,N',N'*-tetraacetic acid acetoxymethyl ester (BAPTA-AM), indomethacin, 2-nitro-4-carboxyphenyl-*N,N*-diphenylcarbonate (NCDC), and SU-1498. The final maximal concentration of DMSO in the perfusion buffer was <0.05%, and this concentration did not have any effect on the basal perfusion pressure in pig skin flaps.

Experimental Protocols

The following protocols were designed to investigate whether VEGF₁₆₅ is a potent vasodilator in the skin vasculature and, if so, what possible receptors and postreceptor signaling pathways and effector mechanism are involved in mediating VEGF₁₆₅-induced vasorelaxation in the pig skin vasculature.

Protocol 1: effect of VEGF₁₆₅ on perfusion pressure in pig skin flaps. The cumulative concentration-dependent decrease in perfusion pressure (i.e., vasorelaxation) induced by VEGF₁₆₅ (5×10^{-16} – 5×10^{-11} M) was studied in pig skin flaps precontracted with NE (5×10^{-6} M), ET-1 (10^{-9} M), or U-46619 (2×10^{-7} M). These submaximal concentrations of drugs were chosen because they were observed in our preliminary study to raise the perfusion pressure of the skin flaps by 40–50 mmHg over the baseline.

The cumulative concentration-dependent decrease in perfusion pressure induced by ACh (10^{-9} – 10^{-4} M) and VEGF₁₆₅ (5×10^{-16} – 5×10^{-11} M) was also studied in skin flaps precontracted with NE (5×10^{-6} M). The EC₅₀ and D₂ values of VEGF₁₆₅ and ACh in NE-precontracted skin flaps were calculated and compared statistically.

Protocol 2: effect of VEGF₁₆₅ on dermal perfusion in pig skin flaps. A dermofluorometry technique was used to investigate the vasorelaxation effect of VEGF₁₆₅ on dermal perfusion in pig skin flaps precontracted with NE (5×10^{-6} M). Total dye fluorescence in pig skin flaps was assessed at the end of the stabilization period (baseline) and 15 min after the infusion of vehicle (control), NE (5×10^{-6} M), or NE and VEGF₁₆₅ (5×10^{-11} M) in pig skin flaps. Results obtained from this study were used to corroborate the vasorelaxation effect of VEGF₁₆₅ in skin flaps assessed by perfusion pressure in the preceding studies.

Protocol 3: role of different tyrosine kinase receptors in triggering VEGF₁₆₅-induced vasorelaxation in pig skin flaps. The perfusion pressure in pig skin flaps was raised with 5×10^{-6} M NE. After stabilization, the cumulative concentration-dependent decrease in perfusion pressure induced by VEGF₁₆₅ (5×10^{-16} – 5×10^{-11} M) was studied in the absence and presence of a specific monoclonal antibody (1 μg/ml) against VEGF receptor-2 (Flk-1/KDR) or a selective VEGF receptor-2 tyrosine kinase inhibitor (5×10^{-6} M SU-1498). The cumulative concentration-dependent vasorelaxation effect of PIGF (5×10^{-16} – 5×10^{-11} M) on perfusion pressure was also studied in pig skin flaps precontracted with 5×10^{-6} M NE. PIGF is known to bind selectively to VEGF receptor-1 (Flt-1) with high affinity but fails to bind to VEGF receptor-2 (3, 36).

Protocol 4: postreceptor signal transduction pathways in VEGF₁₆₅-induced vasorelaxation in pig skin vasculature. Pharmacological probes were used to identify the possible postreceptor signaling pathways in VEGF₁₆₅-induced vasorelaxation in pig skin flaps. The perfusion pressure in pig skin flaps was raised with 5×10^{-6} M NE. After stabilization, the cumulative concentration-dependent relaxation induced by VEGF₁₆₅ (5×10^{-16} – 5×10^{-11} M) was studied in the absence (control) and presence of 5×10^{-6} M of the phos-

pholipase C (PLC) inhibitor NCDC, the inositol 1,4,5-trisphosphate [Ins(1,4,5)P₃] receptor inhibitor 2-APB, the PKC inhibitor chelerythrine, or the intracellular Ca²⁺ chelator BAPTA-AM.

Protocol 5: role of NO and PGI₂ in VEGF₁₆₅-induced vasorelaxation in pig skin vasculature. The perfusion pressure was raised in pig skin flaps with 5×10^{-6} M NE. After stabilization, the cumulative concentration-dependent vasorelaxation induced by VEGF₁₆₅ (5×10^{-16} – 5×10^{-11} M) was studied in the absence (control) and presence of 5×10^{-6} M of the nonspecific NO synthase (NOS) inhibitor L-NNA, the specific inducible NOS (iNOS) inhibitor 1400W, or the specific neuronal NOS (nNOS) inhibitor L-NPA. There is no selective endothelial NOS (eNOS) inhibitor available at the present time.

The concentration-dependent vasorelaxation effect of VEGF₁₆₅ was also studied in the absence and presence of 5×10^{-6} M of the cyclooxygenase inhibitor indomethacin.

In a separate study, the effects of VEGF₁₆₅ on vascular tissue contents of the stable end-products of NO (NO_x) and PGI₂ (6-keto-PGF_{1 α}) were investigated. Specifically, pig skin flaps were perfused for 30 min with buffer (control) and buffer containing 5×10^{-6} M NE or 5×10^{-6} M NE and 5×10^{-11} M VEGF₁₆₅. The arteries and veins from each skin flap were dissected, frozen in liquid nitrogen immediately at the end of each experiment, and stored at -80°C for future assays for the total stable end-products of NO (NO_x) and PGI₂ (6-keto-PGF_{1 α}) in vascular tissue.

Statistics

All values are expressed as means \pm SE unless otherwise stated. The number of observations and the specific statistical tests used in each study are indicated in each figure. Statistical significance was set at $P \leq 0.05$ for all tests.

RESULTS

Effect of VEGF₁₆₅ on Perfusion Pressure in Pig Skin Flaps

VEGF₁₆₅ elicited a cumulative concentration-dependent decrease in perfusion pressure (i.e., vasorelaxation) in pig skin flaps precontracted with NE (5×10^{-6} M), ET-1 (10^{-9} M), or U-46619 (2×10^{-7} M). Vasorelaxation is expressed as a percentage of the perfusion pressure induced by NE, ET-1, or U-46619 (Fig. 1). The maximal vasorelaxation induced by NE, ET-1, and U-46619 was $97 \pm 2\%$, $62 \pm 6\%$, and $55 \pm 2\%$, respectively (Fig. 1).

The vasorelaxation properties of VEGF₁₆₅ and ACh were compared in pig skin flaps precontracted with 5×10^{-6} M NE (Fig. 2). A decrease in perfusion pressure began to occur within 1–2 min after the infusion of ACh or VEGF₁₆₅ was started in the pig skin flap. The time required to achieve a maximal decrease in perfusion pressure for each concentration of ACh or VEGF₁₆₅ was ~ 10 – 15 min. The vasorelaxation potency of VEGF₁₆₅ ($\text{EC}_{50} = 6.2 \pm 4.5 \times 10^{-14}$ M, $\text{pD}_2 = 13.568 \pm 0.314$) was higher ($P < 0.05$) than that of ACh ($\text{EC}_{50} = 1.2 \pm 0.5 \times 10^{-7}$ M, $\text{pD}_2 = 7.076 \pm 0.235$). However, the maximal relaxation was similar between VEGF₁₆₅ ($97 \pm 2\%$) and ACh ($98 \pm 1\%$) (Fig. 2).

Effect of VEGF₁₆₅ on Dermal Perfusion in Pig Skin Flaps Assessed by a Fluorometry Technique

The total dye fluorescence in the vehicle-treated skin flaps (control) was $104 \pm 4\%$ of the baseline (Fig. 3). Perfusion of skin flap with buffer containing 5×10^{-6} M NE reduced the total dye fluorescence to $16 \pm 4\%$ of the baseline. The total dye fluorescence returned to $62 \pm 4\%$ of the baseline when

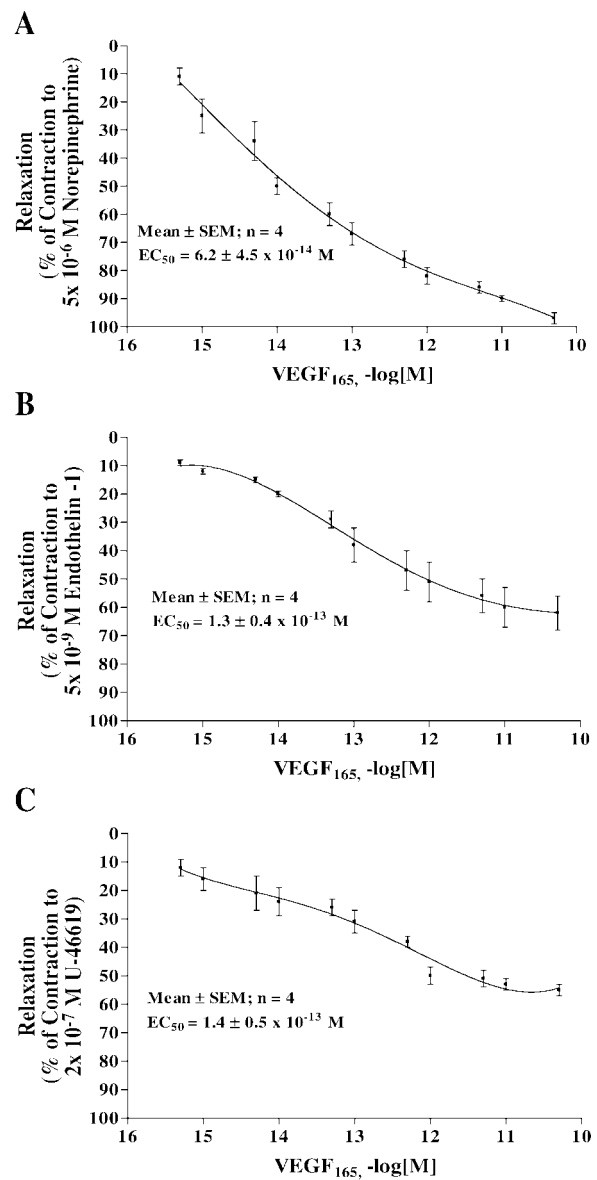


Fig. 1. Cumulative concentration-dependent vasorelaxation induced by VEGF₁₆₅ in isolated perfused skin flaps precontracted with a submaximal concentration of norepinephrine, endothelin-1, or the stable thromboxane A₂ mimetic U-46619.

VEGF₁₆₅ (5×10^{-11} M) was used to induce vasorelaxation in pig skin flaps precontracted with 5×10^{-6} M NE (Fig. 3).

Role of Different Tyrosine Kinase Receptors in Initiating VEGF₁₆₅-Induced Vasorelaxation in Pig Skin Vasculature

VEGF₁₆₅ but not the specific VEGF receptor-1 agonist PIGF elicited cumulative concentration-dependent (5×10^{-16} – 5×10^{-11} M) vasorelaxation in pig skin flaps precontracted with 5×10^{-6} M NE. The concentration-dependent vasorelaxation effect of VEGF₁₆₅ was attenuated significantly ($P < 0.05$) and to a similar extent by a selective VEGF receptor-2 monoclonal antibody ($1 \mu\text{g/ml}$) or the selective VEGF receptor-2 tyrosine kinase inhibitor SU-1498 (5×10^{-6} M) (Fig. 4). The maximal vasorelaxation of VEGF₁₆₅ was reduced ($P < 0.05$) from $97 \pm 2\%$ to $30 \pm 3\%$ and $24 \pm 3\%$ in the presence of a VEGF

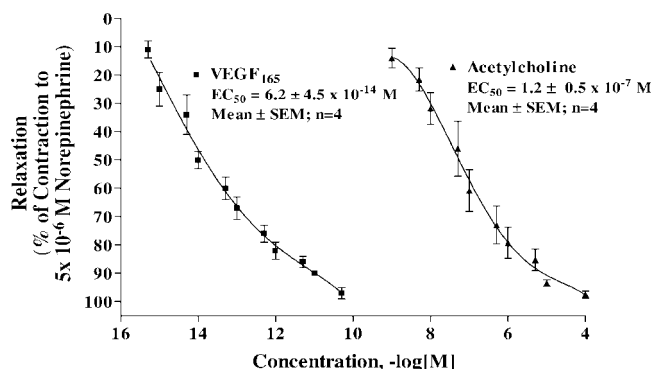


Fig. 2. Cumulative concentration-dependent vasorelaxation effect of VEGF₁₆₅ and acetylcholine in pig skin flaps precontracted with norepinephrine.

receptor-2 antibody or the VEGF receptor-2 tyrosine kinase inhibitor, respectively (Fig. 4).

Postreceptor Signal Transduction Pathways in VEGF₁₆₅-Induced Vasorelaxation in Pig Skin Vasculature

The cumulative concentration-dependent vasorelaxation induced by VEGF₁₆₅ in pig skin flaps precontracted with 5×10^{-6} M NE was reduced significantly ($P < 0.05$) and to a similar extent by 5×10^{-6} M of the PLC inhibitor NCDC, the Ins(1,4,5)P₃ receptor inhibitor 2-APB, the PKC inhibitor chelerythrine, or the intracellular Ca²⁺ chelator BAPTA-AM (Fig. 5). Similarly, the maximal relaxation induced by VEGF₁₆₅ in pig skin flaps precontracted with NE was reduced ($P < 0.05$) from $97 \pm 2\%$ to a similar extent by NCDC ($32 \pm 3\%$), 2-APB ($32 \pm 3\%$), chelerythrine ($39 \pm 4\%$), and BAPTA-AM ($37 \pm 4\%$).

Role of NO and PGI₂ in VEGF₁₆₅-Induced Vasorelaxation in Pig Skin Vasculature

The nonspecific NOS inhibitor L-NNA (5×10^{-6} M) significantly ($P < 0.05$) blocked the concentration-dependent vasorelaxation induced by VEGF₁₆₅ in pig skin flaps precontracted with 5×10^{-6} M NE, and the maximal vasorelaxation was significantly ($P < 0.05$) reduced from $97 \pm 2\%$ to $26 \pm 1\%$. However, the specific iNOS inhibitor 1400W (5×10^{-6} M) and the specific nNOS inhibitor L-NPA (5×10^{-6} M) did

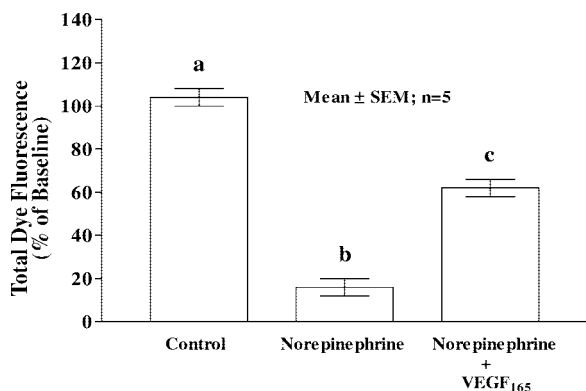


Fig. 3. Effect of VEGF₁₆₅ (5×10^{-11} M) on dermal perfusion of pig skin flaps precontracted with norepinephrine (5×10^{-6} M). Dermal perfusion was assessed by measuring the total dye fluorescence in the skin flap using a dermofluorometry technique. Total dye fluorescence is expressed as a percentage of the baseline. Means without a common letter are significantly different ($a > b > c$, $P < 0.05$) by one-way ANOVA, followed by Tukey's test.

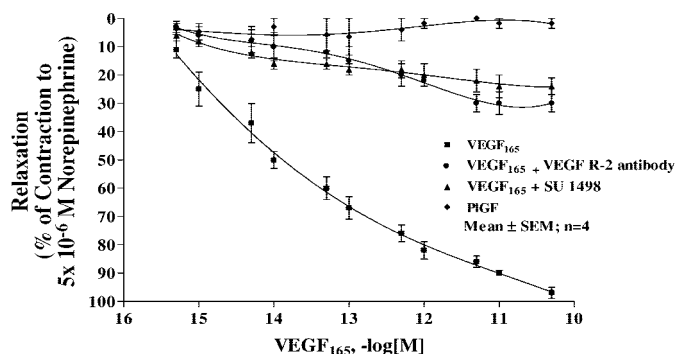


Fig. 4. Role of VEGF₁₆₅ receptor-1 (VEGFR-1) or VEGF₁₆₅ receptor-2 (VEGFR-2) in VEGF₁₆₅-induced vasorelaxation in pig skin flaps. Cumulative concentration-dependent vasorelaxation induced by VEGF₁₆₅ and the specific VEGF receptor-1 agonist placental growth factor (PIGF) were studied in pig skin flaps precontracted with 5×10^{-6} M norepinephrine. The vasorelaxation effect of VEGF₁₆₅ was also studied in the presence of a specific VEGFR-2 antibody (1 μ g/ml) or the specific VEGF receptor-2 tyrosine kinase inhibitor SU-1498 (5×10^{-6} M). PIGF did not elicit any significant vasorelaxation. Vasorelaxation induced by VEGF₁₆₅ was blocked ($P < 0.05$) to a similar extent by a specific VEGFR-2 antibody or SU-1498. Two-way ANOVA with repeated measures was used to compare vasorelaxation between treatment groups.

not have any significant effect on the vasorelaxation induced by VEGF₁₆₅ in pig skin flaps precontracted with NE (Fig. 6).

The cyclooxygenase inhibitor indomethacin elicited a slight but significant ($P < 0.05$) inhibitory effect on the cumulative concentration-dependent vasorelaxation induced by VEGF₁₆₅ in pig skin flaps precontracted with 5×10^{-6} M NE (Fig. 7), and the maximal vasorelaxation was reduced ($P < 0.05$) from $97 \pm 2\%$ to $88 \pm 3\%$.

The total content of stable end-products of NO (NO_x) and PGI₂ (6-keto-PGF_{1 α}) in arteries and veins dissected from pig skin flaps was similar between skin flaps perfused with vehicle (control) or NE (Figs. 8 and 9). Infusion of VEGF₁₆₅ in pig skin flaps constricted with NE significantly increased ($P < 0.01$) the vascular tissue contents of NO_x and 6-keto-PGF_{1 α} by 1.5- and 2.0-fold, respectively, compared with the control (Figs. 8 and 9).

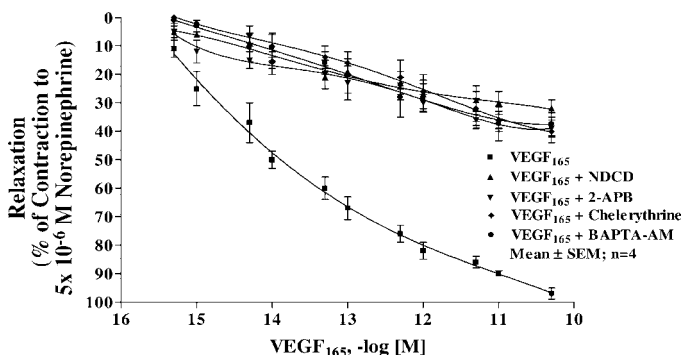


Fig. 5. Postreceptor signal transduction pathways in VEGF₁₆₅-induced vasorelaxation in pig skin flaps. The cumulative concentration-dependent vasorelaxation effect of VEGF₁₆₅ was attenuated to a similar extent by 5×10^{-6} M of the phospholipase C inhibitor 2-nitro-4-carboxyphenyl-*N,N*-diphenylcarbonate (NCDC), the inositol (1,4,5)-trisphosphate receptor inhibitor 2-aminoethoxydiphenylborate (2-APB), the PKC inhibitor chelerythrine, or the intracellular Ca²⁺ chelator 1,2-bis-(2-aminophenoxy)ethane-*N,N,N',N'*-tetraacetic acid acetoxyethyl ester (BAPTA-AM). Two-way ANOVA with repeated measures was used to compare treatment effects on vasorelaxation ($P < 0.05$).

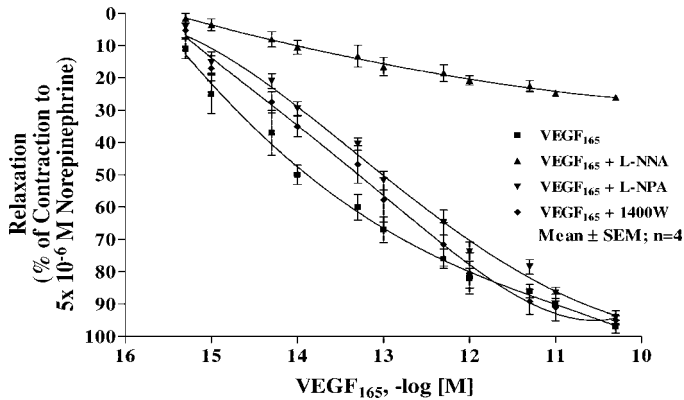


Fig. 6. Role of endothelial (eNOS), neuronal (nNOS), and inducible nitric oxide (iNOS) synthase (iNOS) in VEGF₁₆₅-induced vasorelaxation in pig skin flaps. The cumulative concentration-dependent vasorelaxation induced by VEGF₁₆₅ was significantly blocked in the presence of 5×10^{-6} M of the nonspecific NOS inhibitor *N*^ω-nitro-L-arginine (L-NNA). The vasorelaxation effect of VEGF₁₆₅ was not significantly affected in the presence of 5×10^{-6} M of the specific nNOS inhibitor *N*^ω-propyl-L-arginine (L-NPA) or the specific iNOS inhibitor 1400W. Two-way ANOVA with repeated measures was used to compare treatment effects ($P < 0.05$).

DISCUSSION

Major Findings in the Present Study

Using the isolated perfused pig buttock skin flap model, we investigated for the first time the vascular effects and mechanism of action of acute VEGF₁₆₅ treatment in the skin vasculature. Specifically, we observed that VEGF₁₆₅ is a potent skin vasodilator, thus providing explanation and support for the observation reported by other investigators that acute local subcutaneous/subdermal VEGF₁₆₅ protein or gene therapy effectively reduced ischemic necrosis in skin flap surgery in the rat. In addition, using pharmacological probes, we demonstrated for the first time that VEGF receptor-2 plays an important role in triggering VEGF₁₆₅-induced vasorelaxation in the skin vasculature, and the postreceptor mechanism involves activation of PLC and PKC, an increase in Ins(1,4,5)P₃ activity, a release of the intracellular Ca²⁺ store, and an increase in

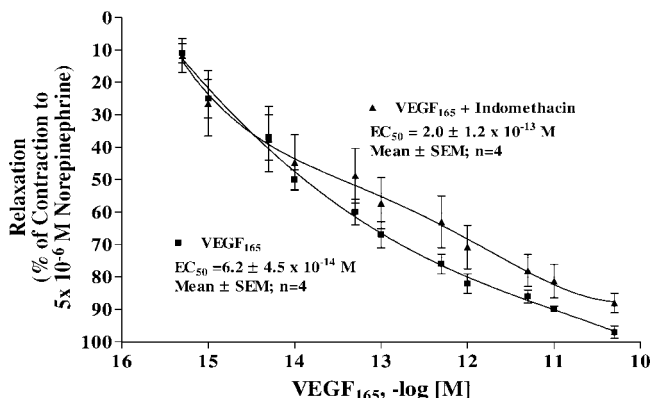


Fig. 7. Role of cyclooxygenase products in VEGF₁₆₅-induced vasorelaxation in pig skin flaps. The cumulative concentration-dependent vasorelaxation effect of VEGF₁₆₅ in pig skin flaps precontracted with 5×10^{-6} M norepinephrine was slightly but significantly attenuated in the presence of 5×10^{-6} M of the cyclooxygenase inhibitor indomethacin. Two-way ANOVA with repeated measures was used to compare treatment effects ($P < 0.05$).

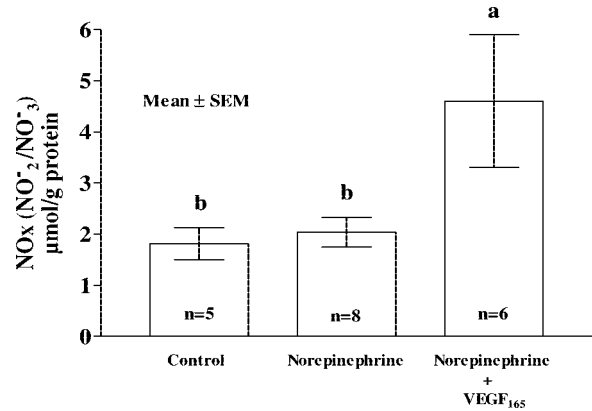


Fig. 8. VEGF₁₆₅-induced NO production in the pig skin vasculature. Pig skin flaps were perfused for 30 min with buffer or buffer containing norepinephrine (5×10^{-6} M) or norepinephrine and VEGF₁₆₅ (5×10^{-11} M). Arteries and veins were dissected from each skin flap for assay of total tissue content of NO ($\text{NO}_x = \text{NO}_2^-/\text{NO}_3^-$). Means without a common letter are significantly different ($a > b$) by one-way ANOVA followed by Tukey's test ($P < 0.05$).

synthesis/release of endothelial NO, which plays a pivotal role in the effector mechanism of VEGF₁₆₅-induced vasorelaxation.

Vasorelaxation Property of VEGF₁₆₅ in Skin Vasculature

There are several lines of evidence from the present study to indicate that acute VEGF₁₆₅ treatment induces potent vasorelaxation in the skin vasculature. Specifically, intra-arterial infusion of VEGF₁₆₅ elicited a potent concentration-dependent vasorelaxation in skin flaps precontracted with a submaximal concentration of NE, ET-1, or U-46619 (Fig. 1). The vasorelaxation potency of VEGF₁₆₅ in the skin vasculature precontracted with U-46619 observed in this study ($\text{EC}_{50} = 1.4 \times 10^{-13}$ M) was similar to that of VEGF₁₆₅ observed in human coronary microvascular rings ($\text{EC}_{50} = 1.0 \times 10^{-13}$ M) precontracted with a submaximal concentration of U-46619 (24). Furthermore, we observed that the vasorelaxation potency of VEGF₁₆₅ ($\text{pD}_2 = 13.568 \pm 0.314$) was significantly higher than that of ACh ($\text{pD}_2 = 7.076 \pm 0.235$) in skin flaps precontracted with a submaximal concentration of NE, and the maximal vasorelaxation for VEGF₁₆₅ and ACh was $97 \pm 2\%$

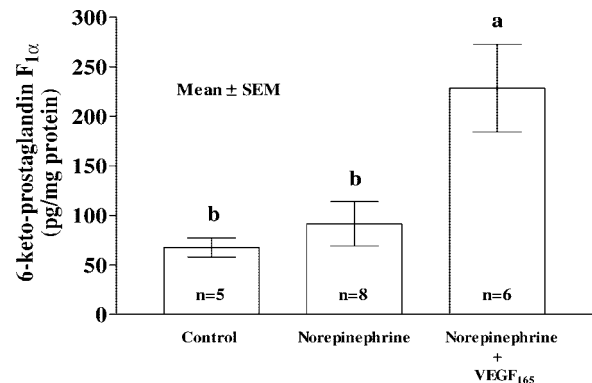


Fig. 9. VEGF₁₆₅-induced prostacyclin (PGI₂) production in the pig skin vasculature. Skin flaps were perfused for 30 min with buffer or buffer containing norepinephrine (5×10^{-11} M). Arteries and veins were dissected from each skin flap for assay of the stable PGI₂ metabolite 6-keto-PGF_{1α}. Means without a common letter are significantly different ($a > b$, $P < 0.05$) by one-way ANOVA followed by Tukey's test ($P < 0.05$).

and $98 \pm 1\%$, respectively (Fig. 2). Vasorelaxation induced by VEGF₁₆₅ or ACh occurred between 1 and 2 min of drug infusion, and the maximal relaxation was reached within 15 min. Last but not least, the acute vasorelaxation effect of VEGF₁₆₅ in NE-constricted skin flaps was confirmed by using a dermofluorometer technique for the assessment of dermal perfusion (Fig. 3).

Role of Different Tyrosine Kinase Receptors in Initiating VEGF₁₆₅-Induced Vasorelaxation in Skin Vasculature

In the past, studies on the functional importance of VEGF receptors were focused on VEGF₁₆₅-induced angiogenesis (16, 25, 26, 29) or vascular permeability (9, 28, 46), but little is known about the role of different VEGF receptors in vasorelaxation. Recently, Li et al. (21) used selective VEGF receptor-1 and VEGF receptor-2 mutants and PIGF, which binds principally to VEGF receptor-1, to investigate for the first time the role of different VEGF receptors in VEGF₁₆₅-induced vasorelaxation in rat aortic rings in organ chambers. They observed that VEGF₁₆₅-induced vasorelaxation involved both VEGF receptor-1 and VEGF receptor-2 but that VEGF receptor-2 was the predominant receptor mediating vasorelaxation in this large conduit vessel. In the present study, PIGF, a monoclonal antibody (1 $\mu\text{g/ml}$) to VEGF receptor-2, and the VEGF receptor-2 tyrosine kinase inhibitor SU-1498 (5×10^{-6} M) were used to evaluate the relative functional importance of VEGF receptor-1 and VEGF receptor-2 in mediating VEGF₁₆₅-induced vasorelaxation in the NE-precontracted skin vasculature in isolated perfused pig skin flaps relevant to skin flap ischemia. We observed that PIGF did not elicit any vasorelaxation effect in the pig skin vasculature precontracted with NE (Fig. 4). On the other hand, the monoclonal antibody to VEGF receptor-2 and SU-1498 blocked the concentration-dependent vasorelaxation effect of VEGF₁₆₅ in the NE-precontracted skin vasculature to a similar extent and reduced the maximum vasorelaxation effect of VEGF₁₆₅ from $97 \pm 2\%$ to $30 \pm 2\%$ and $24 \pm 3\%$, respectively (Fig. 4). These observations indicate that the vasorelaxation effect of VEGF₁₆₅ in the skin vasculature is mediated by VEGF receptor-2, with little or no participation from VEGF receptor-1 in the skin vasculature.

Postreceptor Signal Transduction Pathways in VEGF₁₆₅-Induced Vasorelaxation in Pig Skin Vasculature

In the present study, we used pharmacological probes to investigate the postreceptor signaling pathways in VEGF₁₆₅-induced vasorelaxation in the pig skin vasculature. We observed that the PLC inhibitor NCDC, the Ins(1,4,5)P₃ receptor inhibitor 2-APB, the PKC inhibitor chelerythrine, and the intracellular Ca²⁺ chelator BAPTA-AM blocked the concentration-dependent vasorelaxation effect of VEGF₁₆₅ to a similar extent in pig skin flaps (Fig. 5). These observations led us to speculate that the activation of PLC and PKC and stimulation of Ca²⁺ release from intracellular stores by Ins(1,4,5)P₃ are important postreceptor events in VEGF₁₆₅-induced vasorelaxation in the pig skin vasculature. Interestingly, these pathways are very similar to the signaling pathways in VEGF₁₆₅-induced synthesis/release of NO in cultured vascular segments (44) and endothelial cells (13, 42, 44) reported by other investigators. It was also reported that VEGF₁₆₅ elicited vasorelaxation in endothelium-intact but not endothelium-dis-

rupted vascular rings in organ chambers, and this vasorelaxation effect was blocked by the nonspecific NOS inhibitor N^G-monomethyl-L-arginine or L-NNA (20, 44). In addition, L-NNA also attenuated the increase in coronary blood flow induced by acute VEGF₁₆₅ infusion into the coronary of the pig (23). These observations led us to investigate the role of endothelial NO in the effector mechanism of VEGF₁₆₅-induced vasorelaxation in the pig skin vasculature.

Role of NO and PGI₂ in the Effector Mechanism of VEGF₁₆₅-Induced Vasorelaxation in Pig Skin Flaps

There is evidence from the present studies to indicate that Ca²⁺-dependent eNOS was involved in the synthesis/release of NO, which played a key role in the effector mechanism of VEGF₁₆₅-induced vasorelaxation in the pig skin vasculature. Ca²⁺-dependent eNOS and nNOS and Ca²⁺-independent iNOS are known to stimulate the synthesis/release of NO. Here, we observed that the nonselective NOS inhibitor L-NNA blocked the VEGF₁₆₅-induced concentration-dependent vasorelaxation in pig skin flaps (Fig. 6). However, the selective nNOS inhibitor L-NPA and the selective iNOS inhibitor 1400W did not attenuate the vasorelaxation effect of VEGF₁₆₅ in pig skin flaps (Fig. 6). These observations indicate that VEGF₁₆₅ activates eNOS in the skin vasculature, and eNOS increases the synthesis/release of NO, which causes vasorelaxation. Our speculation is supported by the observation that acute VEGF₁₆₅ treatment increased the tissue content of total NO in the vasculature of pig skin flaps (Fig. 8).

There is evidence to indicate that VEGF₁₆₅ stimulates PGI₂ synthesis/release in endothelial cells (6, 13, 23, 28, 42, 45); thus PGI₂ may also be involved in VEGF₁₆₅-induced vasorelaxation. Indeed, we observed that acute VEGF₁₆₅ treatment induced an increase in vascular tissue contents of the PGI₂ stable metabolite 6-keto-PGF_{1 α} in pig skin flaps (Fig. 9). However, there is evidence in the present study to indicate that NO but not cyclooxygenase products play a major role in VEGF₁₆₅-induced vasorelaxation in pig skin flaps. Specifically, the cyclooxygenase inhibitor indomethacin (5×10^{-6} M) only slightly reduced the concentration-dependent vasorelaxation in pig skin flaps precontracted with 5×10^{-6} M NE. The maximal vasorelaxation was reduced from $97 \pm 2\%$ to $88 \pm 3\%$ (Fig. 7). However, the nonspecific NOS inhibitor L-NNA (5×10^{-6} M) blocked over 70% of the concentration-dependent vasorelaxation effect of VEGF₁₆₅ in pig skin flaps precontracted with the same concentration of NE (Fig. 6).

Effect of VEGF₁₆₅ on Skin Vascular Permeability

It has been reported that NO and PGI₂ also mediate the VEGF₁₆₅-induced increase in vascular permeability in pig coronary venules and guinea pig skin (28, 46). There is evidence from our preliminary study to indicate that VEGF₁₆₅ may also increase vascular permeability in our isolated perfused pig skin flap model. For example, water retention at the end of 2 h of perfusion caused the skin flap to increase in weight by $4.8 \pm 0.5\%$ ($n = 3$) in control skin flaps. Intrarterial infusion of VEGF₁₆₅ (10^{-11} M) caused an increase of $10.9 \pm 2.8\%$ ($n = 3$) in the weight of skin flaps at the end of 2 h of infusion. However, it is unlikely that this increase in water retention (edema) induced by VEGF₁₆₅ may have a significant detrimental effect on vasorelaxation (1, 10). Spe-

cifically, we observed in the present study that vasorelaxation induced by VEGF₁₆₅ completely mitigated NE-induced vasoconstriction in isolated perfused pig skin flaps (Fig. 1A).

However, the effect of a VEGF₁₆₅-induced increase in vascular permeability on the assessment of dermal perfusion by a dermofluorometry technique is unclear at the present time. Specifically, sodium fluorescein dye (C₂₀H₁₀Na₂O₅, mol. wt. 376, Stokes radius 0.45 mm) is used experimentally and clinically as a marker for the indirect assessment of skin perfusion. When injected intravenously, fluorescein dye is carried in the circulation, and it diffuses freely and rapidly from intravascular compartment to extracellular fluid. Fluorescein dye emits fluorescence in the skin, which is visible under ultraviolet light, and the fluorescence can be measured using a dermofluorometer for the indirect assessment of dermal perfusion (43). Recently, it was observed that VEGF₁₆₅ rapidly and transiently increased permeability to fluorescein dye in isolated perfused frog mesenteric microvessels (8). This observation may be interpreted to indicate that VEGF₁₆₅ treatment may cause a transient increase in vascular permeability in the skin flap, and this in turn may increase the rate of fluorescein dye diffusion from microvessels to extravascular fluid. Therefore, the VEGF₁₆₅-induced increase in dermal perfusion assessed by a dermofluorometer is likely the result of both an increase in vascular permeability and vasorelaxation. Because the size of sodium fluorescein is very small and is freely diffusible in normal microvessels, we speculate that the VEGF₁₆₅-induced increase in dermal perfusion measured by a dermofluorometry technique is mainly the result of vasorelaxation rather than the transient increase in vascular permeability.

In summary, we demonstrated for the first time that VEGF₁₆₅ is a potent vasodilator in the skin vasculature. The data obtained thus far indicate that the vasorelaxation effect of VEGF₁₆₅ in the pig skin vasculature is triggered by the activation of VEGF receptor-2, and the postreceptor signaling pathway most likely involves activation of PLC and PKC, an increase in Ins(1,4,5)P₃ activity, a release of the intracellular Ca²⁺ store, and synthesis/release of NO, and PGI₂ and NO plays a predominant role in the effector mechanism of VEGF₁₆₅-induced vasorelaxation in the pig skin vasculature. These findings provide an important insight into the mechanism of action of VEGF₁₆₅ protein or gene therapy in the prevention and/or treatment of skin ischemia in skin flap surgery or skin ischemic diseases.

ACKNOWLEDGMENTS

The authors thank D. McIntyre for word processing in preparation of this manuscript.

GRANTS

This study was supported by Canadian Institutes of Health Research Operating Grant MOP 8048 (to C. Y. Pang). P. D. Addison and M. A. Moses are recipients of the postdoctoral fellowship from the Wharton Endowment Fund to P. C. Neligan.

REFERENCES

1. Acland RD. Experimental skin flap transfer by microvascular anastomosis. In: *Skin Flaps*, edited by Grabb WC and Myers MB. Boston, MA: Little, Brown, 1976, p. 93–106.
2. Black CE, Huang N, Neligan PC, Levine RH, Lipa JE, Lintlop S, Forrest CR, and Pang CY. Effect of nicotine on vasoconstrictor and vasodilator responses in human skin vasculature. *Am J Physiol Regul Integr Comp Physiol* 281: R1097–R1104, 2001.
3. Cao Y, Chen H, Zhou L, Chiang MK, Anand-Apte B, Weatherbee JA, Wang Y, Fang F, Flanagan JG, and Tsang MLS. Heterodimers of placenta growth factor/vascular endothelial growth factor. *J Biol Chem* 271: 3154–3162, 1996.
4. Daniel RK and Kerrigan CL. The omnipotential pig buttock skin flap. *Plast Reconstr Surg* 70: 11–16, 1982.
5. Daniel RK and Kerrigan CL. Principles and physiology of skin flap surgery. In: *Plastic Surgery*, edited by McCarthy JG. Philadelphia, PA: Saunders, 1990, vol. 1, p. 225–378.
6. Davidge ST, Baker PN, McLaughlin MK, and Roberts JM. Nitric oxide produced by endothelial cells increase production of eicosanoids through activation of prostaglandin H synthase. *Circ Res* 77: 274–283, 1995.
7. Forrest CR, Pang CY, Zhong AG, and Kreidstein ML. Efficacy of intravenous infusion of prostacyclin (PGI₂) or prostaglandin E₁ (PGE₁) in augmentation of skin flap blood flow and viability in the pig. *Prostaglandins* 41: 537–558, 1991.
8. Fu BM and Shen S. Structural mechanism of acute VEGF effect on microvessel permeability. *Am J Physiol Heart Circ Physiol* 284: H2124–H2135, 2003.
9. Gille H, Kowalski J, Li B, Le Couter J, Moffat B, Zioncheck TF, Pelletier N, and Ferrara N. Analysis of biological effects and signaling properties of Flt-1 (VEGFR-1) and KDR (VEGFR-2). *J Biol Chem* 276: 3222–3230, 2001.
10. Grabb WC. Introduction to the clinical aspects of skin flaps. In: *Skin Flaps*, edited by Grabb WC and Myers MB. Boston, MA: Little, Brown, 1975, p. 135–143.
11. Grabb WC. Techniques in plastic surgery. In: *Plastic Surgery*, edited by WC Grabb and Smith JW. Boston: Little, Brown, 1986, p. 3–74.
12. Gurunluogly Ozer KR, Skugor B, Lubiowski P, Carnevale K, and Siemionow M. Effect of transfection time on the survival of epigastric skin flaps pretreated with adenovirus encoding the VEGF gene. *Ann Plast Surg* 49: 161–169, 2002.
13. He H, Venema VJ, Gu X, Venema RC, Marrero MB, and Caldwell RB. Vascular endothelial growth factor signals endothelial cell production of nitric oxide and Prostacyclin through Flk-1/KDR activation of c-Src. *J Biol Chem* 274: 25130–25135, 1999.
14. He W, Neligan P, Lipa JE, Forrest CR, and Pang CY. Comparison of secondary ischemic tolerance between pedicled and free island buttock skin flaps in the pig. *Plast Reconstr Surg* 100: 72–81, 1997.
15. Jeremy JY, Dashwood MR, Mehta D, Izzat MB, Shukla N, and Angelini GD. Nitric oxide, prostacycline and cyclic nucleotide formation in externally stented porcine vein grafts. *Atherosclerosis* 141: 297–305, 1998.
16. Kanno S, Oda N, Abe M, Terai Y, Ito M, Shitara K, Tabayashi K, Shibuya M, and Sato Y. Roles of two VEGF receptors. Flt-1 and KDR in the signal transduction of VEGF effects in human vascular endothelial cells. *Oncogene* 19: 2138–2146, 2000.
17. Kerrigan CL and Daniel RK. Critical ischemia time and the failing skin flap. *Plast Reconstr Surg* 69: 986–989, 1982.
18. Krum JM, Mani N, and Rosenstein JM. Angiogenic and astroglial response to vascular endothelial growth factor administration in adult rat brain. *Neuroscience* 110: 589–604, 2002.
19. Kryger Z, Zhang F, Dogan T, Cheng C, Lineaweaver WC, and Buncke HJ. The effects of VEGF on survival of a random flap in the rat: examination of various routes of administration. *Br J Plast Surg* 53: 234–239, 2000.
20. Ku DD, Zaleski JK, Liu S, and Brock TA. Vascular endothelial growth factor induces EDRF-dependent relaxation in coronary arteries. *Am J Physiol Heart Circ Physiol* 265: H586–H592, 1993.
21. Li B, Ogasawara AK, Wei W, He GW, Zioncheck TF, Bunting S, de Vos AM, and Jin H. KDR (VEGF receptor 2) is the major mediator for the hypotensive effect of VEGF. *Hypertension* 39: 1095–1100, 2002.
22. Liu MH, Jin H, Floten S, Ren Z, Yin APC, and He GW. Vascular endothelial growth factor-mediated endothelium-dependent relaxation in human internal mammary artery. *Ann Thorac Surg* 73: 819–824, 2002.
23. Lopez JJ, Lahan RJ, Carrozza JP, Rofukuji M, Selke FW, Bunting S, and Simons M. Hemodynamic effects of intracoronary VEGF delivery: evidence of tachyphylaxis and NO dependence of response. *Am J Physiol Heart Circ Physiol* 273: H1317–H1323, 1997.
24. Metais C, Li J, Simons M, and Sellke FW. Effects of coronary artery disease on expression and microvascular response to VEGF. *Am J Physiol Heart Circ Physiol* 275: H1411–H1418, 1998.

25. Meyer M, Clauss M, Lepple-Weinhues Waltenberrger J, Augustin HG, Ziche M, Lanz C, Buttner M, Rziha HJ, and Dehio C. A novel vascular endothelial growth factor encoded by Orf virus, VEGF-E, mediates angiogenesis via signaling through VEGFR-2 (KDR) but not VEGFR-1 (Flt-1) receptor tyrosine kinase. *EMBO J* 18: 363–374, 1999.
26. Millauer B, Wizigmann-Voos S, Schnurch H, Martinez R, Moller NPH, Risau W, and Ullrich A. High-affinity VEGF binding and development expression suggest Flk-1 as a major regulator of vasculogenesis and angiogenesis. *Cell* 72: 835–846, 1993.
27. Monteiro-Riviere NA, Baynes RE, and Riviere JE. Pyridostigmine bromide modulates topical irritant-induced cytokine release from human epidermal keratinocytes and isolated perfused porcine skin. *Toxicology* 183: 15–28, 2003.
28. Murohara T, Horowitz JR, Silver M, Tsurumi Y, Chen D, Sullivan A, and Isner JM. Vascular endothelial growth factor/vascular permeability factor enhances vascular permeability via nitric oxide and prostacyclin. *Circulation* 97: 99–107, 1998.
29. Murphy JF and Fitzgerald DJ. Vascular endothelial cell growth factor (VEGF) induces cyclooxygenase (COX)-dependent proliferation of endothelial cells (EC) via the VEGF-2 receptor. *The FASEB Journal* 15: 1667–1669, 2001.
30. O'Toole G, MacKenzie D, Lindeman R, Buckley MF, Marucci D, McCarthy N, and Poole M. Vascular endothelial growth factor gene therapy in ischemic rat skin flaps. *Br J Plast Surg* 55: 55–58, 2002.
31. Padubidri A and Browne E. Effect of vascular endothelial growth factor on survival of random extension of axial pattern skin flaps in the rat. *Ann Plast Surg* 37: 604–611, 1996.
32. Pang CY, Forrest CR, and Morris SF. Pharmacologic augmentation of skin flap viability: a hypothesis to mimic the surgical delay phenomenon or a wishful thought. *Ann Plast Surg* 22: 293–306, 1989.
33. Pang CY, Xu H, Huang N, Forrest CR, Perreault TM, and Neligan P. Amplification effect and mechanism of action of endothelin-1 in U 46619-induced vasoconstriction in pig skin. *Am J Physiol Regul Integr Comp Physiol* 280: R713–R720, 2001.
34. Pang CY, Yang RZ, Neligan P, Xu N, Chiu C, Zhong A, and Forrest CR. Vascular effects and mechanism of action of endothelin-1 in isolated perfused pig skin. *J Appl Physiol* 79: 2106–2113, 1995.
35. Pang CY, Zhang J, Xu H, Lipa JE, Forrest CR, and Neligan P. Role and mechanism of endothelin-B receptors in mediating ET-1-induced vasoconstriction in pig skin. *Am J Physiol Regul Integr Comp Physiol* 275: R1066–R1074, 1998.
36. Park JE, Chen HH, Winer J, Houck KA, and Ferrara N. Placenta growth factor: potentiation of vascular endothelial growth factor bioactivity in vitro and in vivo and high affinity binding to Flt-1/KDR. *J Biol Chem* 269: 25646–25654, 1994.
37. Pu LLQ, Ahmed S, Thomson JG, Reid MA, Madsen JA, and Restifo RJ. Endothelial cell growth factor enhances musculocutaneous flap survival through the process of neovascularization. *Ann Plast Surg* 42: 306–312, 1999.
38. Randall MD, Edwards DH, and Griffin TM. Activities of endothelin-1 in the vascular network of the rabbit ear: a microangiographic study. *Br J Pharmacol* 101: 781–788, 1990.
39. Riviere JE. Isolated perfused porcine skin flap system. *Pharm Biotechnol* 8: 387–407, 1996.
40. Riviere JE, Bowman KF, Monteiro-Riviere NA, Dix LP, and Caver MP. The isolated perfused porcine skin flap (IPPSF). A novel model for percutaneous absorption and cutaneous toxicology studies. *Fund Appl Toxicol* 7: 444–453, 1986.
41. Selke FW, Wang SY, Stamler CV, Lopez JJ, Li J, Li J, and Simons M. Enhances microvascular relaxations to VEGF and bFGF in chronically ischemic porcine myocardium. *Am J Physiol Heart Circ Physiol* 271: H713–H720, 1996.
42. Shen BQ, Lee DY, and Zioncheck TF. Vascular endothelial growth factor governs endothelial nitric oxide synthase expression via a KDR/Flk-1 receptor and a protein kinase C signaling pathway. *J Biol Chem* 274: 3305–3063, 1999.
43. Thomson JG and Kerrigan CL. Dermofluorometry: thresholds for predicting flap survival. *Plast Reconstr Surg* 83: 839–864, 1989.
44. Van-der-Zee R, Murohara T, Luo Z, Zollmann F, Passeri J, Lekutat C, and Isner JM. Vascular endothelial growth factor/vascular permeability factor augments nitric oxide release from quiescent rabbit and human vascular endothelium. *Circulation* 95: 1030–1037, 1997.
45. Wheeler-Jones C, Abu-Ghazaleh R, Cospedal R, Houliston RA, Martin J, and Zachary I. Vascular endothelial growth factor stimulates Prostacyclin production and activation of cytosolic phospholipase A₂ in endothelial cells via p42/44 mitogen-activated protein kinase. *FEBS letters* 420: 28–32, 1997.
46. Wu HM, Yuan Y, Zawieja DC, Tinsley J, and Granger HJ. Role of phospholipase C, protein kinase C, and calcium in VEGF-induced venular hyperpermeability. *Am J Physiol Heart Circ Physiol* 276: H535–H542, 1999.
47. Xuan YT, Tang XL, Qiu Y, Banerjee S, Takano H, Han H, and Bolli R. Biphasic response of cardiac NO synthase isoforms to ischemic preconditioning in conscious rabbits. *Am J Physiol Heart Circ Physiol* 279: H2360–H2371, 2000.